JOURNAL OF GUIDANCE, CONTROL, AND DYNAMICS
Vol. 15, No. 3, May-June 1992

Finite Element Method for Optimal Guidance of an Advanced Launch Vehicle

Dewey H. Hodges,* Robert R. Bless,* Anthony J. Calise,† and Martin Leung‡
Georgia Institute of Technology, Atlanta, Georgia 30332

A temporal finite element based on a mixed form of Hamilton's weak principle is summarized for optimal control problems. The resulting weak Hamiltonian finite element method is extended to allow for discontinuities in the states and/or discontinuities in the system equations. An extension of the formulation to allow for control inequality constraints is also presented. The formulation does not require element quadrature, and it produces a sparse system of nonlinear algebraic equations. To evaluate its feasibilty for real-time guidance applications, this approach is applied to the trajectory optimization of a four-state, two-stage model with inequality constraints for an advanced launch vehicle. Numerical results for this model are presented and compared to results from a multiple-shooting code. The results show the accuracy and computational efficiency of the finite element method.

Introduction

FUTURE space transportation and deployment needs are critically dependent on the development of reliable and economical launch vehicles that will provide flexible, routine access to orbit. The current Space Shuttle represents an effort to build one vehicle to serve many roles. The Space Shuttle is largely autonomous in its on-orbit, deorbit, and entry through landing guidance. However, an extensive amount of ground support is required to prepare the guidance system for launch. Thus, future launch systems will require onboard algorithms that maximize system performance as measured by autonomy, mission flexibility, in-flight adaptability, reliability, accuracy, and payload capability. They must be computationally efficient, robust, self-starting, and capable of functioning independently of ground control. Also, the algorithms must be designed with the anticipation that the launch vehicle will undergo evolutionary growth.[1]

One approach to optimal guidance consists of repeatedly solving a two-point boundary-value problem that results from the traditional necessary conditions for optimality in an optimal control problem formulation. The vehicle state at discrete instants of time along a trajectory can be viewed as a new starting condition, and the remainder of the trajectory is reoptimized for that condition. The open-loop optimal control is applied for a short interval of time, and feedback is introduced by reoptimization at the next time instant. This process presupposes that the two-point boundary-value problem can be reliably solved in a time interval that is small compared with the control update interval. Knowledge of the previous solution helps in providing a good starting point for the optimization process; however, no method has been demonstrated that can operate reliably in a real-time environment.

In Ref. 2, a weak formulation for the solution of optimal control problems was derived based on Hamilton's weak principle. The so-named weak Hamiltonian finite element formulation was derived in such a way that very crude shape functions could be employed, thus eliminating the need for element numerical quadrature (even for the most nonlinear of problems). Furthermore, the formulation was presented with such generality that one could solve *any* optimal control problem belonging to the class of problems considered simply by providing the various elements of the performance index and the proper boundary conditions. The versatility, accuracy, and ease in implementing the formulation was demonstrated in two examples of elementary trajectory optimization. For these reasons, it is believed that the weak Hamiltonian formulation holds significant advantages over other finite element techniques.[3,4]

In this paper, the weak formulation is developed further, allowing for an even broader class of problems to be solved. We begin by presenting a summary of the weak formulation presented in Ref. 2. Next, the formulation is extended to handle discontinuities and control inequality constraints. A model of an advanced launch vehicle (ALV) is then presented and numerical results are presented herein. The numerical results are compared with a multiple-shooting code as a check on the accuracy of the solution. Of particular interest is the performance in terms of execution time and accuracy vs the number of elements used to represent the time span of the trajectory.

Weak Principle for Optimal Control

A weak formulation for optimal control problems with continuous state, costate, and control histories is presented in Ref. 2. Therein, it is shown that the formulation weakly (i.e., in a variational sense) satisfies the Euler-Lagrange equations and boundary conditions that have already been established in optimal control theory.[5] The derivation begins with a performance index taken from Eq. (2.8.4) of Ref. 5. The first variation of the performance index is taken in a standard manner with states and controls having arbitrary variations. Also, all strong boundary conditions are transformed into natural or "weak" boundary conditions by adjoining a constraint equation to the performance index with an unknown Lagrange multiplier. The final weak form is then obtained by integration of this equation by parts in such a way that no time derivatives of states or costates appear. The advantages of the weak formulation are that 1) no numerical quadrature is required, 2) the nonlinear algebraic equations possess a very sparse Jaco-

Received July 31, 1990; revision received March 8, 1991; accepted for publication March 18, 1991.

*Professor, School of Aerospace Engineering. Associate Fellow AIAA.

*Professor, School of Aerospace Engineering. Associate Fellow AIAA.

†Graduate Research Assistant, School of Aerospace Engineering; currently, Research Engineer, Lockheed Engineering and Sciences Company, Hampton, Virignia 23666. Member AIAA.

‡Graduate Research Assistant, School of Aerospace Engineering. Student Member AIAA.

bian, and 3) the resulting algebraic equations are easily programmed and can be solved very quickly, especially when sparsity is exploited.

Although many practical problems in optimal control theory can be solved by using the weak formulation described in Ref. 2, there are problems that require more generality. Specifically, the weak formulation must be extended to allow for discontinuities (in the states and/or system equations) and inequality constraints placed on the controls and states. Discontinuities might arise when finding the optimal trajectory of a multistage rocket. At the time the first stage is dropped, the mass state would suffer a discontinuity. Furthermore, the thrust of the rocket (one of the system parameters) would also change at this staging time, thereby creating a discontinuity in the system equations. These discontinuities produce jumps in the states, costates, and possibly the control variables.

The theory to extend the weak formulation to handle problems with discontinuities is described next. The inclusion of control inequality constraints is outlined in this paper; however, greater details and an example of the use of the method are given in Ref. 6. Because additional conditions are necessary for optimality when state constraints are present,[7] the theory for state constraints along with examples will be presented in a later paper.

Theory for State Discontinuities

The derivation of the weak formulation to include state discontinuities (or jumps) and discontinuities in the system equations is similar to the derivation in Ref. 2; however, special care must be taken because of the unknown staging time. Therefore, the details of the derivation are presented below for a problem with one discontinuity. Of course, the extension of the formulation to problems with multiple discontinuities is possible and should not present special difficulties.

Consider a problem with one discontinuity where the time of discontinuity will be called the staging time and denoted by t_s. The formulation must be modified to accommodate the unknown staging time t_s, the constraint on the states at t_s (as opposed to a constraint on the states at the final time), the jump in the states at t_s, the jump in the costates at t_s, the change in state equations at t_s (due to the change in system parameters), and finally the transversality condition to find t_s. Furthermore, the control u may be discontinuous at the staging time.

Now, let a system be defined by a set of n states x and a set of m controls u. Furthermore, let the system be governed by a set of state equations of the form $\dot{x}=f_I(x,u,t)$ before t_s and $\dot{x}=f_{II}(x,u,t)$ after t_s. Elements of the performance index J_0 may be denoted with integrands $L_I(x,u,t)$ before t_s, $L_{II}(x,u,t)$ after t_s, a function $\phi[x(t_0),x(t_f),t_0,t_f]$, where the initial and final times are denoted by t_0 and t_f, and a function $\phi_s[x(t_s^-),x(t_s^+),t_s]$, where t_s^- and t_s^+ denotes instants just before and after the staging time t_s, respectively. In addition, any constraints imposed on the states and time at t_0 and t_f may be placed in a set of functions $[x(t_0),x(t_f)t_0,t_f]$, whereas constraints imposed at t_s^- and t_s^+ may be placed in $[x(t_s^-),x(t_s^+),t_s]$. These constraints may be adjoined to the performance index by discrete Lagrange multipliers ν and ν_s, respectively. Finally, the state equations may be adjoined to the performance index with a set of Lagrange multiplier functions $\lambda(t)$ that will be referred to as costates. For notational convenience, we define $\Phi=\phi+\nu^T\psi$ and $\Phi_s=\phi_s+\nu_s^T\psi_s$. For variables t_s and t_f, this yields a performance index of the form

$$J_0=\int_{t_0}^{t_s^-}\left[L_I+\lambda^T(f_I-\dot{x})\right]\mathrm{d}t + \int_{t_s^+}^{t_f}\left[L_{II}+\lambda^T(f_{II}-\dot{x})\right]\mathrm{d}t+\Phi_s+\Phi \tag{1}$$

The constraint equations to be adjoined to the performance index to transform the strong boundary conditions to weak ones are simply that the states be continuous at the initial and final times.[2] Introducing

$$x_0=x|_{t_0}\triangleq\lim_{t\to t_0^+}x(t) \quad \text{and} \quad x_f=x|_{t_f}\triangleq\lim_{t\to t_f^-}x(t) \tag{2}$$

and

$$\hat{x}_0=\hat{x}|_{t_0}\triangleq x(t_0) \quad \text{and} \quad \hat{x}_f=\hat{x}|_{t_f}\triangleq x(t_f) \tag{3}$$

continuity is weakly enforced by adjoining $\alpha^T(x-\hat{x})|_{t_0}^{t_f}$ to J_0 where α is a set of discrete unknown Lagrange multipliers defined only at t_0 and t_f. The new performance index is

$$J=\int_{t_0}^{t_s^-}\left[L_I+\lambda^T(f_I-\dot{x})\right]\mathrm{d}t+\int_{t_s^+}^{t_f}\left[L_{II}+\lambda^T(f_{II}-\dot{x})\right]\mathrm{d}t + \Phi_s+\Phi+\alpha^T(x-\hat{x})\Big|_{t_0}^{t_f} \tag{4}$$

Now, denote with $\delta(\ )$ the variation of ( ) when holding time fixed, and let $\mathrm{d}(\ )$ be the variation of ( ) when time is allowed to vary. The fixed and free-time variations at $t=t_0$ and $t=t_f$ are related by[5,8]

$$\delta x(t_0)=\mathrm{d}x(t_0) \quad \text{and} \quad \delta x(t_f)=\mathrm{d}x(t_f)-\dot{x}|_{t_f}\,\mathrm{d}t_f \tag{5}$$

and similarly for λ. (Note that t_0 is considered to be a fixed time so that $\mathrm{d}t_0=0$.) The free and fixed-time variations at $t=t_s^-$ and $t=t_s^+$ are related by

$$\delta x(t_s^-)=\mathrm{d}x(t_s^-)-\dot{x}|_{t_s^-}\,\mathrm{d}t_s \tag{6a}$$

and

$$\delta x(t_s^+)=\mathrm{d}x(t_s^+)-\dot{x}|_{t_s^+}\,\mathrm{d}t_s \tag{6b}$$

and similarly for λ. It is noted that if a particular state (or costate) does not have a discontinuity at $t=t_s$, then the corresponding free-time variation is continuous at t_s, i.e. $\mathrm{d}x(t_s^-)=\mathrm{d}x(t_s^+)$. Now, proceeding with the development of the weak form, the first variation of J is taken and the $\delta\dot{x}$ term appearing in both integrands is integrated by parts. The resulting equation is

$$\begin{aligned}\mathrm{d}J=&\int_{t_0}^{t_s^-}\left[\delta L_I+\delta f_I^T\lambda+\delta\lambda^T(f_I-\dot{x})+\delta x^T\dot{\lambda}\right]\mathrm{d}t-\delta x^T\lambda\Big|_{t_0}^{t_s^-}\\&+\int_{t_s^+}^{t_f}\left[\delta L_{II}+\delta f_{II}^T\lambda+\delta\lambda^T(f_{II}-\dot{x})+\delta x^T\dot{\lambda}\right]\mathrm{d}t-\delta x^T\lambda\Big|_{t_s^+}^{t_f}\\&+\delta\nu_s^T\psi_s+\delta\nu^T\psi+\mathrm{d}x^T\left(\frac{\partial\Phi_s}{\partial x}\right)^T\Bigg|_{t_s^-}^{t_s^+}\\&+\mathrm{d}x^T\left(\frac{\partial\Phi}{\partial x}\right)^T\Bigg|_{t_0}^{t_f}+\delta\alpha^T(x-\hat{x})\Big|_{t_0}^{t_f}+\alpha^T(\mathrm{d}x-\mathrm{d}\hat{x})\Big|_{t_0}^{t_f}\\&+\mathrm{d}t_f\left[L_{II}+\lambda^T(f_{II}-\dot{x})+\frac{\partial\Phi}{\partial t_f}\right]\Bigg|_{t_f}\\&+\mathrm{d}t_s\Bigg\{\left[L_I+\lambda^T(f_I-\dot{x})\right]\Big|_{t_s^-}\\&-\left[L_{II}+\lambda^T(f_{II}-\dot{x})\right]\Big|_{t_s^+}+\frac{\partial\Phi_s}{\partial t_s}\Bigg\}\end{aligned} \tag{7}$$

A necessary condition for an extremal of J is that the first variation be zero. Also, the admissible variations of the states are chosen to be continuous at the initial and final times and therefore $(\mathrm{d}x-\mathrm{d}\hat{x})|_{t_0}^{t_f}=0$. For notational convenience, define $H_I = L_I + \lambda^T f_I$, $H_{II} = L_{II} + \lambda^T f_{II}$, and

$$\hat{\lambda}_0 = \hat{\lambda}\big|_{t_0} = \frac{\partial \Phi}{\partial x}\bigg|_{t_0} \quad \text{and} \quad \hat{\lambda}_f = \hat{\lambda}\big|_{t_f} = \frac{\partial \Phi}{\partial x}\bigg|_{t_f} \tag{8}$$

Finally, by using Eqs. (5) and (6) to eliminate δx at t_0, t_s^-, t_s^+, and t_f, Eq. (7) can be simplified with the use of Eq. (8), to

$$\int_{t_0}^{t_s^-} \left\{ \delta\lambda^T(f_I - \dot{x}) + \delta x^T\left[\dot{\lambda} + \left(\frac{\partial H_I}{\partial x}\right)^T\right] + \delta u^T\left(\frac{\partial H_I}{\partial u}\right)^T \right\} \mathrm{d}t$$
$$+ \int_{t_s^+}^{t_f} \left\{ \delta\lambda^T(f_{II} - \dot{x}) + \delta x^T\left[\dot{\lambda} + \left(\frac{\partial H_{II}}{\partial x}\right)^T\right] \right.$$
$$\left. + \delta u^T\left(\frac{\partial H_{II}}{\partial u}\right)^T \right\} \mathrm{d}t + \delta \nu_s^T \psi_s + \delta\nu^T\psi$$
$$+ \mathrm{d}x^T\left[\left(\frac{\partial \Phi_s}{\partial x}\right)^T + \lambda\right]\Bigg|_{t_s^-}^{t_s^+} + \mathrm{d}x^T(\hat{\lambda} - \lambda)\Bigg|_{t_0}^{t_f} + \delta\alpha^T(x - \hat{x})\Bigg|_{t_0}^{t_f}$$
$$+ \mathrm{d}t_f\left(H_{II} + \frac{\partial \Phi}{\partial t_f}\right)\Bigg|_{t_f} + \mathrm{d}t_s\left(H_I\Big|_{t_s^-} - H_{II}\Big|_{t_s^+} + \frac{\partial \Phi_s}{\partial t_s}\right) = 0 \tag{9}$$

It is easily verified that the necessary conditions for an extremal of J, as defined in Ref. 5, are contained in the coefficients of the virtual quantities [i.e., the δ( ) and d( ) terms] of Eq. (9). This is described in Ref. 2, and thus only the new boundary conditions that appear as the result of the staging are discussed here. Specifically, the requirement for the coefficient of $\delta\nu_s$ to vanish yields Eq. (3.7.3) of Ref. 5. The requirement for the coefficient of $\mathrm{d}x|_{t_s^-}$ to vanish yields Eq. (3.7.11), whereas the requirement for the coefficient of $\mathrm{d}x|_{t_s^+}$ to vanish yields Eq. (3.7.12). Finally, the coefficient of $\mathrm{d}t_s$ is the transversality condition in Eq. (3.7.13).

Having satisfied the requirement that none of the fundamental equations are altered, the weak formulation may now be derived. First, we choose $\delta\alpha = \mathrm{d}\lambda$ as described in Ref. 2. Next, the $\dot{x}$ and $\dot{\lambda}$ terms in Eq. (9) are integrated by parts. Also, Eq. (5) is used to eliminate $\mathrm{d}x$ and $\mathrm{d}\lambda$ at t_0 and t_f. The resulting equation is

$$\int_{t_0}^{t_s^-} \left[\delta\lambda^T f_I + \delta\dot{\lambda}^T x - \delta\dot{x}^T\lambda + \delta x^T\left(\frac{\partial H_I}{\partial x}\right)^T + \delta u^T\left(\frac{\partial H_I}{\partial u}\right)^T \right] \mathrm{d}t$$
$$+ \int_{t_s^+}^{t_f} \left[\delta\lambda^T f_{II} + \delta\dot{\lambda}^T x - \delta\dot{x}^T\lambda + \delta x^T\left(\frac{\partial H_{II}}{\partial x}\right)^T \right.$$
$$\left. + \delta u^T\left(\frac{\partial H_{II}}{\partial u}\right)^T \right] \mathrm{d}t + \delta\nu_s^T\psi_s + \delta\nu^T\psi + \delta x^T\hat{\lambda}\Bigg|_{t_0}^{t_f}$$
$$- \delta\lambda^T\hat{x}\Bigg|_{t_0}^{t_f} + \mathrm{d}x^T\left[\left(\frac{\partial \Phi_s}{\partial x}\right)^T + \lambda\right]\Bigg|_{t_s^-}^{t_s^+} + \delta\lambda^T x\Bigg|_{t_s^-}^{t_s^+} - \delta x^T\lambda\Bigg|_{t_s^-}^{t_s^+}$$
$$+ \mathrm{d}t_f\left(H_{II} + \frac{\partial \Phi}{\partial t}\right)_f\Bigg|_{t_f} + \mathrm{d}t_s\left(H_I\Big|_{t_s^-} - H_{II}\Big|_{t_s^+} + \frac{\partial \Phi_s}{\partial t_s}\right) = 0 \tag{10}$$

Note that an $\dot{x}^T(\hat{\lambda} - \lambda)|_{t_f}$ term and a $\dot{\lambda}^T(x - \hat{x})|_{t_f}$ term should appear in the $\mathrm{d}t_f$ equation, but these terms are each zero in accordance with the natural boundary conditions [see the $\mathrm{d}x$ and $\delta\alpha$ coefficients in Eq. (9)]. Equation (6) is now used to eliminate $\mathrm{d}x$ at t_s^- and t_s^+. Again, the natural boundary conditions in Eq. (9) must be used to avoid changing the $\mathrm{d}t_s$ coefficient. The weak principle is now given as

$$\int_{t_0}^{t_s^-} \left[\delta\lambda^T f_I + \delta\dot{\lambda}^T x - \delta\dot{x}^T\lambda + \delta x^T\left(\frac{\partial H_I}{\partial x}\right)^T + \delta u^T\left(\frac{\partial H_I}{\partial u}\right)^T \right] \mathrm{d}t$$
$$+ \int_{t_s^+}^{t_f} \left[\delta\lambda^T f_{II} + \delta\dot{\lambda}^T x - \delta\dot{x}^T\lambda + \delta x^T\left(\frac{\partial H_{II}}{\partial x}\right)^T \right.$$
$$\left. + \delta u^T\left(\frac{\partial H_{II}}{\partial u}\right)^T \right] \mathrm{d}t + \delta x^T\hat{\lambda}\Bigg|_{t_0}^{t_f} - \delta\lambda^T\hat{x}\Bigg|_{t_0}^{t_f}$$
$$+ \delta x^T\left(\frac{\partial \Phi_s}{\partial x}\right)^T\Bigg|_{t_s^-}^{t_s^+} + \delta\lambda^T x\Bigg|_{t_s^-}^{t_s^+} + \delta\nu^T\psi + \delta\nu_s^T\psi_s$$
$$+ \mathrm{d}t_s\left(H_I\Big|_{t_s^-} - H_{II}\Big|_{t_s^+} + \frac{\partial \Phi_s}{\partial t_s}\right) + \mathrm{d}t_f\left(H_{II} + \frac{\partial \Phi}{\partial t_f}\right)\Bigg|_{t_f} = 0 \tag{11}$$

This is the governing equation for the weak Hamiltonian method for optimal control problems of the form specified. It will serve as the basis for the finite element discretization described next for constructing candidate solutions (i.e., solutions that satisfy all of the necessary conditions).

Finite Element Discretization

Because of the staging, the finite element discretization must be handled slightly differently than it was in Ref. 2. Therefore, for clarity, full details of the discretization are given. Let the time interval from t_0 to t_s^- be broken into N_1 elements and the time interval from t_s^+ to t_f be broken into N_2 elements. For notational convenience, define $N = N_1 + N_2$. The nodal values of time for these elements are t_i for $i = 1, 2, \ldots, N+1$ where $t_0 = t_1$, $t_s = t_{N_1+1}$, and $t_f = t_{N+1}$. A nondimensional elemental time τ is defined as

$$\tau = \frac{t - t_i}{t_{i+1} - t_i} = \frac{t - t_i}{\Delta t_i} \tag{12}$$

Since one derivative of δx and $\delta\lambda$ appears in Eq. (11), linear shape functions for δx and $\delta\lambda$ may be chosen. Since no derivatives of x or λ appear, then piecewise constant shape functions for x and λ are chosen. These shape functions are taken to be

$$\delta x = \delta x_i^+(1 - \tau) + \delta x_{i+1}^-\tau \tag{13}$$

and

$$x = \begin{cases} \hat{x}_i^+ & \text{if } \tau = 0 \\ \bar{x}_i & \text{if } 0 < \tau < 1 \\ \hat{x}_{i+1}^- & \text{if } \tau = 1 \end{cases} \tag{14}$$

and similarly for $\delta\lambda$ and λ. The superscripted plus and minus signs signify values just before and after the subscripted nodal value. For all nodes *except* the $N_1 + 1$ node that corresponds to t_s, the values for x and λ, as well as for δx and $\delta\lambda$, are equal on either side of the node. Furthermore, it is important to understand that $\hat{x}_1^+ = \hat{x}_0 = x(t_0)$, $\hat{\lambda}_1^+ = \hat{\lambda}_0 = \lambda(t_0)$, $\hat{x}_{N+1}^- = \hat{x}_f = x(t_f)$, and $\hat{\lambda}_{N+1}^- = \hat{\lambda}_f = \lambda(t_f)$. We can choose $u = \bar{u}_i$ and $\delta u = \delta\bar{u}_i$ as shape functions for the control and its variation since these quantities are never differentiated with respect to time.

Plugging in the shape functions described for x, λ, and u, substituting $t = t_i + \tau\Delta t_i$, and carrying out the integration over τ from 0 to 1, a general algebraic form of the Hamiltonian weak form for optimal control problems is obtained. The algebraic equations are

$$\sum_{i=1}^{N_1} \left\{ \delta x_i^{+T}\left[\bar{\lambda}_i + \frac{\Delta t_i}{2}\left(\frac{\partial \bar{H}_I}{\partial \bar{x}}\right)_i^T\right] - \delta\lambda_i^{+T}\left[\bar{x}_i - \frac{\Delta t_i}{2}(\bar{f}_I)_i\right] \right.$$
$$- \delta x_{i+1}^{-T}\left[\bar{\lambda}_i - \frac{\Delta t_i}{2}\left(\frac{\partial \bar{H}_I}{\partial \bar{x}}\right)_i^T\right] + \delta\lambda_{i+1}^{-T}\left[\bar{x}_i + \frac{\Delta t_i}{2}(\bar{f}_I)_i\right]$$
$$\left. + \delta\bar{u}_i^T\left[\Delta t_i\left(\frac{\partial \bar{H}_I}{\partial \bar{u}}\right)_i^T\right]\right\} + \mathrm{d}t_s\left(\hat{H}_{N_1+1}^- - \hat{H}_{N_1+1}^+ + \frac{\partial \Phi_s}{\partial t_s}\right)$$
$$- \delta x_1^{+T}\hat{\lambda}_1^+ + \delta\lambda_1^{+T}\hat{x}_1^+ + \delta x_{N_1+1}^{+T}\left(\frac{\partial \Phi_s}{\partial x}\right)^{+T} + \delta\lambda_{N_1+1}^{+T}\hat{x}_{N_1+1}^{+T}$$

$$
\begin{aligned}
&- \delta x_{N_1+1}^{-T}\left(\frac{\partial \Phi_s}{\partial x}\right)^{-T} - \delta\lambda_{N_1+1}^{-T}\hat{x}_{N_1+1}^{-T} \\
&+ \sum_{i=N_1+1}^{N}\left\{\delta x_i^{+T}\left[\bar{\lambda}_i + \frac{\Delta t_i}{2}\left(\frac{\partial \bar{H}_{II}}{\partial \bar{x}}\right)_i^T\right]\right. \\
&- \delta\lambda_i^{+T}\left[\bar{x}_i - \frac{\Delta t_i}{2}(\bar{f}_{II})_i\right] - \delta x_{i+1}^{-T}\left[\bar{\lambda}_i - \frac{\Delta t_i}{2}\left(\frac{\partial \bar{H}_{II}}{\partial \bar{x}}\right)_i^T\right] \\
&\left.+ \delta\lambda_{i+1}^{-T}\left[\bar{x}_i + \frac{\Delta t_i}{2}(\bar{f}_{II})_i\right] + \delta\bar{u}_i^T\left[\Delta t_i\left(\frac{\partial \bar{H}_{II}}{\partial \bar{u}}\right)_i^T\right]\right\} \\
&+ \mathrm{d}t_f\left(\hat{H}_{N+1} + \frac{\partial \Phi}{\partial t_f}\right) - \delta\lambda_{N+1}^{-T}\hat{x}_{N+1}^{-} + \delta x_{N+1}^{-T}\hat{\lambda}_{N+1}^{-} \\
&+ \delta\nu_s^T\psi_s + \delta\nu^T\psi = 0 \qquad (15)
\end{aligned}
$$

where $\bar{H} = H(\bar{x},\bar{u},\bar{t})$, $\hat{H} = H(\hat{x},\hat{u},\hat{t})$, and $\bar{t}$ and $\hat{t}$ represent the value of the time either at the interior of an element or at a node itself. Note that there are not only boundary conditions at t_0 and t_f but also additional boundary conditions at the staging time t_s, namely the coefficients of $\delta x_{N_1+1}^{-}$, $\delta x_{N_1+1}^{+}$, $\delta\lambda_{N_1+1}^{-}$, and $\delta\lambda_{N_1+1}^{+}$. This is where the jumps in the states and costates are allowed to occur.

Equation (15) is a system of nonlinear algebraic equations. The coefficient of each arbitrary virtual quantity (δx, $\delta\lambda$, δu, $\mathrm{d}t_s$, $\mathrm{d}t_f$, $\delta\nu_s$, and $\delta\nu$) must be set equal to zero to satisfy Eq. (15). However, not all of the previous virtual quantities are independent. As stated earlier, $\delta x_i^+ = \delta x_i^-$ for all i except $i = N_1 + 1$, which is the node number corresponding to the staging time. At this node, it was observed from the calculus of variations that the virtual quantities suffer a discontinuity. Now, the coefficients of $\delta x_{N_1+1}^-$ and $\delta x_{N_1+1}^+$ may be treated as separate equations; however, a different option has been chosen in an attempt to provide uniformity to the equations to be programmed. Define

$$\delta x_{N_1+1}^- = \delta x_{N_1+1} + \delta\eta_\lambda \qquad (16)$$

and

$$\delta x_{N_1+1}^+ = \delta x_{N_1+1} - \delta\eta_\lambda \qquad (17)$$

When these values are substituted into Eq. (15), then two new arbitrary virtual quantities appear, namely δx_{N_1+1} and $\delta\eta_\lambda$. Figure 1 helps clarify the assembly process of the virtual states. The figure shows three straight lines depicting linear shape functions over three elements. For the nonjump node N_1, the virtual quantities are equal at the node and replaced with δx_{N_1}. At the jump node, however, $\delta x_{N_1+1}^+$ and $\delta x_{N_1+1}^-$ are replaced with an average value δx_{N_1+1}. Another virtual quantity $\delta\eta_\lambda$ also appears but is not shown in Fig. 1. The coefficient of δx_{N_1+1} is now of the same form as all of the other δx terms and the $\delta\eta_\lambda$ coefficient contains an equation to extract the needed nodal value of λ at t_s, namely $\hat{\lambda}_{N_1+1}^-$. To simplify matters further though, the coefficient of $\delta\eta_\lambda$ can be replaced with a still simpler expression to extract the needed nodal value. This expression comes from the recursive equation

$$\hat{z}_{i+1} = 2\bar{z}_i - \hat{z}_i \qquad (18)$$

which is derivable from application of Eq. (15) to a single-stage, single-element system. Here z represents either the state x or the costate λ. The first nodal value $\hat{z}_1$ is equal to the initial values of the states and costates that are represented by $\hat{x}_1^+$ and $\hat{\lambda}_1^+$ in Eq. (15). The same process is done with the $\delta\lambda_{N_1+1}^-$ and $\delta\lambda_{N_1+1}^+$ terms so that a $\delta\lambda_{N_1+1}$ and $\delta\eta_x$ are introduced. As a final step, all superscript plus and minus signs can be dropped, except on $\hat{x}_{N_1+1}$ and $\hat{\lambda}_{N_1+1}$ since these values are distinct. The algebraic equations now take the form

$$
\begin{aligned}
&\sum_{i=1}^{N_1}\left\{\delta x_i^T\left[\bar{\lambda}_i + \frac{\Delta t_i}{2}\left(\frac{\partial \bar{H}_I}{\partial \bar{x}}\right)_i^T\right] - \delta\lambda_i^T\left[\bar{x}_i - \frac{\Delta t_i}{2}(\bar{f}_I)_i\right]\right. \\
&\quad - \delta x_{i+1}^T\left[\bar{\lambda}_i - \frac{\Delta t_i}{2}\left(\frac{\partial \bar{H}_I}{\partial \bar{x}}\right)_i^T\right] + \delta\lambda_{i+1}^T\left[\bar{x}_i + \frac{\Delta t_i}{2}(\bar{f}_I)_i\right] \\
&\quad \left.+ \delta\bar{u}_i^T\left[\Delta t_i\left(\frac{\partial \bar{H}_I}{\partial \bar{u}}\right)_i^T\right]\right\} + \mathrm{d}t_s\left(\hat{H}_{N_1+1}^- - \hat{H}_{N_1+1}^+ + \frac{\partial \Phi_s}{\partial t_s}\right) \\
&\quad - \delta x_1^T\hat{\lambda}_1 + \delta\lambda_1^T\hat{x}_1 + \delta x_{N_1+1}^T\left[\left(\frac{\partial \Phi_s}{\partial x}\right)^{+T} - \left(\frac{\partial \Phi_s}{\partial x}\right)^{-T}\right] \\
&\quad + \delta\lambda_{N_1+1}^T(\hat{x}_{N_1+1}^+ - \hat{x}_{N_1+1}^-) \\
&\quad + \sum_{i=N_1+1}^{N}\left\{\delta x_i^T\left[\bar{\lambda}_i + \frac{\Delta t_i}{2}\left(\frac{\partial \bar{H}_{II}}{\partial \bar{x}}\right)_i^T\right] - \delta\lambda_i^T\left[\bar{x}_i - \frac{\Delta t_i}{2}(\bar{f}_{II})_i\right]\right. \\
&\quad - \delta x_{i+1}^T\left[\bar{\lambda}_i - \frac{\Delta t_i}{2}\left(\frac{\partial \bar{H}_{II}}{\partial \bar{x}}\right)_i^T\right] + \delta\lambda_{i+1}^T\left[\bar{x}_i + \frac{\Delta t_i}{2}(\bar{f}_{II})_i\right] \\
&\quad \left.+ \delta\bar{u}_i^T\left[\Delta t_i\left(\frac{\partial \bar{H}_{II}}{\partial \bar{u}}\right)_i^T\right]\right\} + \mathrm{d}t_f\left(\hat{H}_{N+1} + \frac{\partial \Phi}{\partial t_f}\right) \\
&\quad - \delta\lambda_{N+1}^T\hat{x}_{N+1} + \delta x_{N+1}^T\hat{\lambda}_{N+1} + \delta\nu_s^T\psi_s + \delta\nu^T\psi \\
&\quad + \delta\eta_x\left\{\hat{x}_{N_1+1}^- - (-1)^{N_1}\left[\hat{x}_1 + 2\sum_{k=1}^{N_1}(-1)^k\bar{x}_k\right]\right\} \\
&\quad + \delta\eta_\lambda\left\{\hat{\lambda}_{N_1+1}^- - (-1)^{N_1}\left[\hat{\lambda}_1 + 2\sum_{k=1}^{N_1}(-1)^k\bar{\lambda}_k\right]\right\} = 0 \qquad (19)
\end{aligned}
$$

Equation (19) may be used to solve optimal control problems that suffer a discontinuity in the trajectory. Often in practical applications, these algebraic equations may be simplified slightly to minimize the number of unknown variables. Consider the case (as will be seen in the example) where ψ_s is a scalar function of one variable at t_s^- and t_s^+, i.e, there is a known jump in one of the states.

More specifically, since the jump in the states expressed as $\hat{x}_{N_1+1}^- - \hat{x}_{N_1+1}^+$ is known, then the coefficient of $\delta\lambda_{N_1+1}$ will be replaced with an actual numerical value, such as the drop mass of a booster rocket stage. Also, Φ_s^- would be retained to define the unknown staging time, but Φ_s^+ would be set to zero since the jump has already been solved for. Then the jump in the

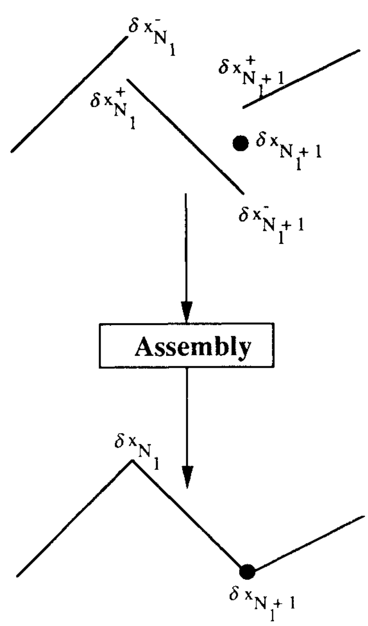

Fig. 1 Assembly of virtual states.

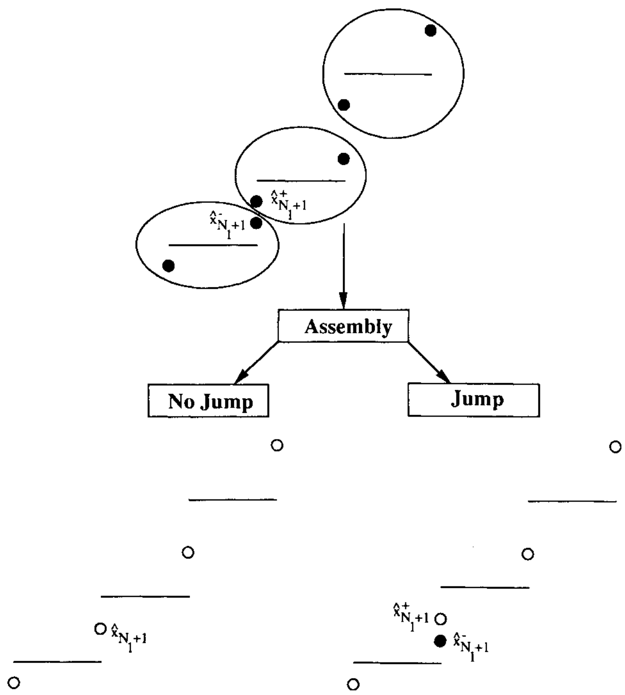

Fig. 2 Assembly of states.

costates may be defined as

$$\hat{\lambda}^-_{N_1+1} - \hat{\lambda}^+_{N_1+1} = \frac{\partial \Phi_s^{-\,T}}{\partial x} \tag{20}$$

To use Eq. (19), one would let $\hat{x}^-_{N_1+1}$ and $\hat{\lambda}^-_{N_1+1}$ be the unknown variables and then replace $\hat{x}^+_{N_1+1}$ (from the physical jump condition) and $\hat{\lambda}^+_{N_1+1}$ [from Eq. (20)] in terms of other unknowns. Note that if there is no jump condition on a particular state or costate, then the nodal values just before and after staging are equal. Figure 2 helps clarify this process. In Fig. 2 are shown three piecewise constant shape functions spanning three elements. The solid black circles in the top half of the figure represent the hatted or nodal values of the states at the beginning and end of the element. Note that only the jump node is labeled. After assembly, two conditions can occur. If there is no jump, then the nodal values from the left and right sides are equal and do not appear in the algebraic equations. These "disappearing" nodal values are represented by the hollow circles in the lower half of the figure. [Values are recoverable there by use of Eq. (18).] If there is a jump, then the nodal values $\hat{x}^+_{N_1+1}$ and $\hat{x}^-_{N_1+1}$ are *not* equal, but only $\hat{x}^-_{N_1+1}$ is treated as an unknown (represented by the solid black dot) and $\hat{x}^+_{N_1+1}$ is eliminated from the equations in terms of $\hat{x}^-_{N_1+1}$. Thus it is now one of the "disappearing" nodal values also and depicted by a hollow circle.

In addition, one must introduce the optimality condition ($\partial H/\partial u = 0$) at t_s^- and t_s^+ to solve for the values of the control u just before and after the staging time. (Note that the optimality condition could be adjoined to the performance index initially, rather than introducing this equation separately.) Finally, the coefficient of the $\mathrm{d}t_s$ equation (i.e., the continuity of the Hamiltonian) gives the extra equation to solve for the unknown staging time t_s.

Also, as was noted in Ref. 2, for most problems the initial conditions are given for all n states and thus, in accordance with Eq. (8), all the initial costates are unknown. Therefore, instead of treating elements of ν at $t = t_0$ as unknowns and replacing $\hat{\lambda}|_{t_0}$ with these unknowns, we will instead treat $\hat{\lambda}|_{t_0}$ as unknowns and eliminate the $\delta\nu|_{t_0}$ equations from the weak principle.

It may be instructive to count the number of equations and unknowns for a given problem. Consider a problem with n states, m controls, one constraint on the states at t_s, and q_2 constraints on the states at t_f. There will be N_1 elements in the first stage and N_2 elements in the second stage. The given boundary conditions will be for $\hat{x}_0$ and $\hat{\lambda}_f$. The number of unknowns is $2n$ (for $\hat{\lambda}_0$ and $\hat{x}_f$) $+2n(N_1+N_2)$ (for $\bar{x}_i$ and $\hat{\lambda}_i$ in the first and second stages) $+2n$ (for $\hat{x}^-_{N_1+1}$ and $\hat{\lambda}^-_{N_1+1}$) $+m(N_1+N_2)$ (for $\bar{u}_i$ in the first and second stages) $+3m$ (for $\hat{u}$ at t_s^-, t_s^+, and t_f) $+1$ (for ν_s) $+q_2$ (for ν) $+2$ (for t_s and t_f). The number of equations is $2n(N_1+N_2+1)$ (for $\delta\bar{x}_i$ and $\delta\hat{\lambda}_i$) $+2n$ (for $\delta\eta_x$ and $\delta\eta_\lambda$) $+m(N_1+N_2)$ (for $\delta\bar{u}_i$) $+3m$ (for $\partial H/\partial u = 0$ at t_s^-, t_s^+, and t_f) $+1$ (for $\delta\nu_s$) $+q_2$ (for $\delta\nu$) $+2$ (for $\mathrm{d}t_s$ and $\mathrm{d}t_f$). Thus, the number of equations and unknowns is the same. Remember that the solution of these equations is an approximate solution of the necessary conditions. One must still perform second-order calculations (i.e., $\partial^2 H/\partial u^2$) to test for a minimum or maximum.

Theory for Control Inequality Constraints

Consider a system of n states x and m controls u defined by $\dot{x} = f(x,u,t)$. Suppose that g is a $p \times 1$ column matrix of control constraints of the form $g(x,u,t) \le 0$. One way of handling inequality constraints is to use a "slack" variable.[9] The idea is that if $g \le 0$ then g plus some positive number (i.e., the slack variable) is equal to zero. Thus denoting the slack variable by k^2, then the following $p \times 1$ column matrices for K and δK, the variation of K, may be defined:

$$K = \lfloor k_1^2 \quad k_2^2 \quad \dots \quad k_p^2 \rfloor^T$$
$$\delta K = \lfloor 2k_1\delta k_1 \quad 2k_2\delta k_2 \quad \dots \quad 2k_p\delta k_p \rfloor^T \tag{21}$$

The constraint now becomes $g(x,u,t) + K = 0$ and will be adjoined to the performance index by using p Lagrange multiplier functions $\mu(t)$.

The new performance index with the constraint equations on the states adjoined so that all strong boundary conditions are transformed into natural boundary conditions is

$$J = \int_{t_0}^{t_f} \left[L(x,u,t) + \lambda^T(f - \dot{x}) + \mu^T(g + K) \right] \mathrm{d}t + \Phi + \alpha^T(x - \hat{x})\big|_{t_0}^{t_f} \tag{22}$$

Once again the weak principle is derived in an analogous manner as given earlier. The details of the derivation and an example showing the explicit use of the formulation are given in Ref. 6.

Denoting the variations of the variables at the initial and final times with subscripts 0 and f, then the resulting equation is

$$\begin{aligned}
&\int_{t_0}^{t_f} \Bigg\{ -\delta\dot{x}^T\lambda + \delta\lambda^T f + \delta\dot{\lambda}^T x + \delta x^T \left[\left(\frac{\partial L}{\partial x}\right)^T + \left(\frac{\partial f}{\partial x}\right)^T \lambda + \left(\frac{\partial g}{\partial x}\right)^T \mu \right] + \delta u^T \left[\left(\frac{\partial L}{\partial u}\right)^T + \left(\frac{\partial f}{\partial u}\right)^T \lambda + \left(\frac{\partial g}{\partial u}\right)^T \mu \right] \\
&\quad + \delta\mu^T(g + K) + \delta K^T \mu \Bigg\} \mathrm{d}t + \delta t_f \left(L + \lambda^T f + \frac{\partial\phi}{\partial f} + \nu^T \frac{\partial\psi}{\partial f} \right)\Bigg|_{t_f} + \delta\nu^T\psi \\
&\quad + \delta x_f^T \hat{\lambda}_f - \delta x_0^T \hat{\lambda}_0 - \delta\lambda_f^T \hat{x}_f + \delta\lambda_0^T \hat{x}_0 = 0
\end{aligned} \tag{23}$$

Note that in Eq. (23) a value for u is required at t_f. To obtain u, one must also find the values of K and μ at t_f. These unknowns are found by setting the coefficients of δu_f, δK_f^T, and $\delta\mu_f^T$ equal to zero in the following:

$$\delta u_f^T\left[\left(\frac{\partial L}{\partial u}\right)^T+\left(\frac{\partial f}{\partial u}\right)^T\lambda+\left(\frac{\partial g}{\partial u}\right)^T\mu\right]\Bigg|_{t_f}$$

$$\delta\mu_f^T(g+K)|_{t_f}$$

$$\delta K_f^T\mu|_{t_f} \tag{24}$$

Equation (23) is the governing equation for the weak Hamiltonian method that includes inequality constraints on the controls. The next step is to introduce constant shape functions within each element for k and μ:

$$k=\bar{k}_i, \qquad \mu=\bar{\mu}_i$$

$$\delta k=\delta\bar{k}_i, \qquad \delta\mu=\delta\bar{\mu}_i \tag{25}$$

These shape functions (along with the ones described earlier) may be substituted into Eq. (23). The integration may be done by inspection to obtain a set of algebraic equations. Note that there are an additional Np unknown $\bar{k}$ and Np unknown $\bar{\mu}$, along with $2Np$ extra equations (from the δK and $\delta\mu$ coefficients). Thus, the number of equations and unknowns is still the same.

Finally, note that if a given problem has discontinuities *and* control constraints, then the theory described earlier may be combined to solve the problem. Thus, one breaks the time line into two or more pieces, adjoins the control constraint(s) to each integral, and finally derives the governing equations as before.

Model for an Advanced Launch Vehicle

In this section, a model is presented that is suitable for evaluating the usefulness of the weak Hamiltonian finite element approach to real time guidance of an ALV. A two-stage, four-state vehicle is considered that has two control inequality constraints and one state constraint.

We confine our attention to vertical plane dynamics of a vehicle flying over a spherical, nonrotating Earth. This results in the following model for the states m (mass), h (height), V (velocity), and γ (flight-path angle):

$$\dot{m}=-\frac{T_{vac}}{gI_{sp}}$$

$$\dot{h}=V\sin\gamma$$

$$\dot{V}=\frac{T\cos\alpha-D}{m}-\frac{\mu\sin\gamma}{r^2}$$

$$\dot{\gamma}=\left(\frac{T\sin\alpha+L}{mV}\right)+\left(\frac{V}{r}-\frac{\mu}{r^2V}\right)\cos\gamma \tag{26}$$

where T is the thrust, D the drag, and L the lift. Here α, the angle of attack, has been adopted as a control variable.

The aerodynamic, propulsion, and atmospheric models are given by the following equations:

$$T=T_{vac}-A_e p(h), \qquad M=\frac{V}{a(h)}$$

$$r=R_e+h, \qquad q=\frac{\rho V^2}{2}$$

$$D=qSC_D(M,\alpha), \qquad L=qSC_L(M,\alpha) \tag{27}$$

The atmospheric data for density ρ, pressure p, and speed of sound a are obtained from Ref. 10.

The vehicle parameters chosen for this model are

$$S_I=131.34\ \text{m}^2, \qquad S_{II}=65.67\ \text{m}^2$$

$$T_{vac_I}=25{,}813{,}400\ \text{N}, \qquad T_{vac_{II}}=7{,}744{,}020\ \text{N}$$

$$A_{e_I}=37.515\ \text{m}^2, \qquad A_{e_{II}}=11.254\ \text{m}^2$$

$$I_{sp_I}=I_{sp_{II}}=430.0\ \text{s} \tag{28}$$

where subscripts I and II refer to the first and second stages, respectively.

The aerodynamic coefficient data C_D and C_L are defined as functions of the Mach number M and angle of attack α.[11] The physical constants used in the preceding model are the Earth's gravitational constant $\mu=3.9906\times10^{14}$ m^3s^{-2}, the Earth's mean radius $R_e=6.378\times10^6$ m, and the acceleration due to gravity $g=9.81$ ms^{-2}.

The three constraints are:

$$g_1(x,u,t)=\alpha q-2925\ \text{rad-Pa}\le 0$$

$$g_2(x,u,t)=-(\alpha q+2925)\ \text{rad-Pa}\le 0$$

$$q(h,V)-40{,}698.2\ \text{Pa}\le 0 \tag{29}$$

None of these constraints are violated. However, the first will be enforced with smaller values of its upper band.

The continuous and discrete elements of the performance index are

$$L_I=L_{II}=0, \qquad \phi=m|t_f \tag{30}$$

and the final time t_f is open. The initial conditions specified are $m(0)=1.52345\times10^6$ kg, $h(0)=400$ m, $V(0)=64.48941$ m/s, and $\gamma(0)=89.5$ deg. The final conditions are $h(t_f)=148{,}160.0$ m, $V(t_f)=7858.1995$ m/s, and $\gamma(t_f)=0.0$ deg. The burnout mass of the first stage is 645,500 kg and the drop mass of the booster is 98,880 kg.

The finite element equations are solved by a Newton-Raphson method. An explicit Jacobian is formed and the sparse matrix solver as coded in Ref. 12 is used at each iteration. Initial guesses were obtained in a trial-and-error manner. By relaxing the initial and final conditions on the states, a solution was obtained for a small number of elements. Then, new solutions were obtained as the initial conditions were slowly brought back to the prescribed conditions. Finally, initial guesses for a higher number of elements were found by interpolating the results from a solution based on a smaller number of elements.

Results

In Figs. 3-10, numerical results for the ALV model with no constraints enforced are given for 2, 4, and 8 elements per time interval, where the number of elements is denoted by $(N_1\!:\!N_2)$ on the plots. These results are compared to a multiple-shooting code[13] as a check on the accuracy of the method and of the program. For the unconstrained case, the state histories are shown in Figs. 3-6 and the costate histories are shown in Figs. 7-10. For all cases, the (8:8) run lies on the essentially exact curve corresponding to the multiple-shooting (MS) code. In general, even the (4:4) run yields an excellent approximation to the solution.

The control time history is shown in Fig. 11. It is seen from this graph that although the (8:8) run is close to the exact curve, it has not converged on the answer. Because of the large slopes and sharp peaks in the control, the finite element method required 16 elements in the first stage to converge on the solution. However, it is important to note that accurate results are still obtained with only eight elements in the second

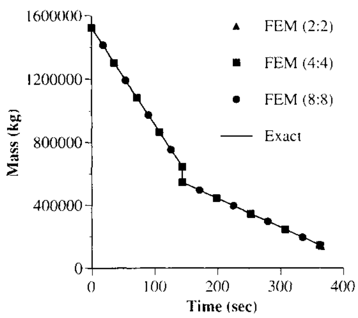

Fig. 3 Mass vs time.

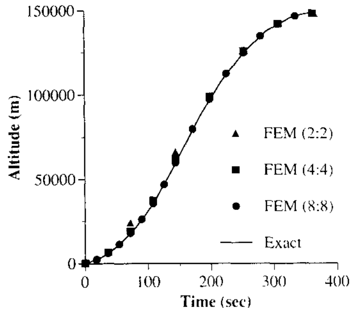

Fig. 4 Altitude vs time.

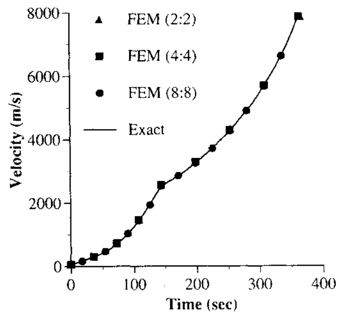

Fig. 5 Velocity vs time.

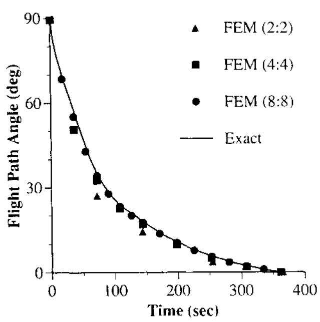

Fig. 6 Flight path angle vs time.

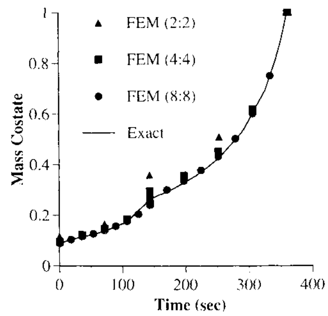

Fig. 7 Mass costate vs time.

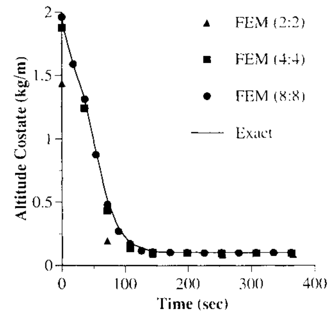

Fig. 8 Altitude costate vs time.

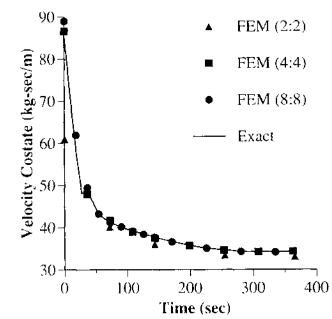

Fig. 9 Velocity costate vs time.

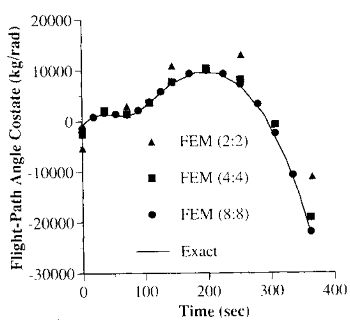

Fig. 10 Flight path angle costate vs time.

stage. Thus it is possible to cluster elements as required to refine the solution.

As a feel for the global convergence of the method, the Hamiltonian of the unconstrained system is plotted in Fig. 12 for 2, 4, 8, and 16 elements per stage. Convergence toward the exact answer of zero with an increase in the number of elements is easily seen.

Figure 13 shows a graph of αq. (The dynamic pressure q is not shown because it does not violate the constraint.) It can be seen clearly that the control constraint, g_1, is close to being violated. This is the only constraint that was added to the program to generate the next two graphs.

In Figs. 14 and 15, the control constriant ($g_1 = \alpha q - 2925.0$) has been included in the finite element formulation. For academic purposes, the unconstrained case and two unrealistic constraints are presented. Even for the most severe constraint, the time histories for the states, costates, and dynamic pressure and the value of the performance index are virtually unchanged. Also, no significant extra computer time was expended.

The (4:4) results for the constrained case were obtained in 1.1 CPU s on a SUN 4/370. This time represents the solution of 112 simultaneous nonlinear equations. The corresponding Jacobian is composed of 91.5% zeroes. The (8:8) results were found in 2.0 CPU s. This represents the solution of 200 equations whose Jacobian matrix contains 94.8% zeroes. Five iterations were required with a Newton-Raphson method to converge on the solution for both cases. Of course, the number of

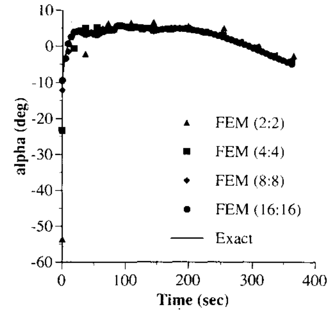

Fig. 11 Angle of attack α vs time.

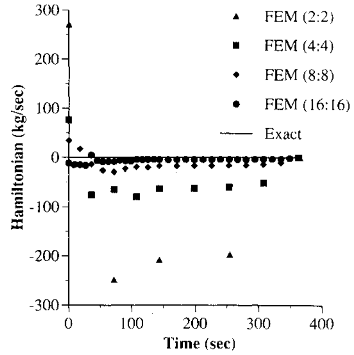

Fig. 12 Hamiltonian vs time.

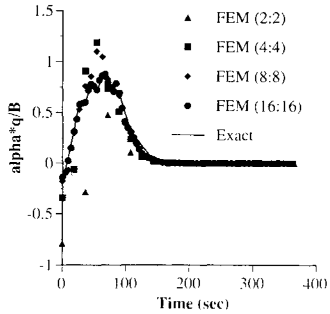

Fig. 13 αq vs time.

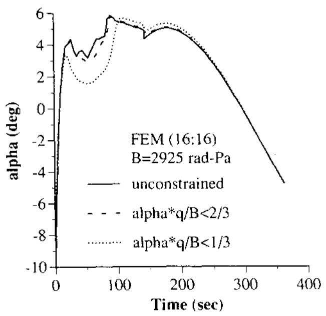

Fig. 14 Angle of attack α vs time for various levels of αq constraint.

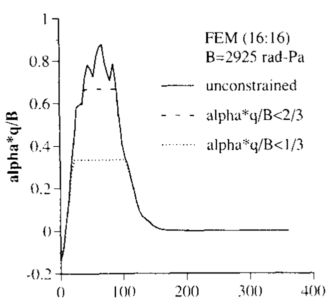

Fig. 15 αq vs time for various levels of αq constraint.

iterations depends on the quality of the initial guesses. In an onboard computational setting, the initial guesses should be quite good since they would probably be determined from a previously obtained solution. Therefore, real-time guidance may be realizable with this solution procedure.

Conclusions

In this paper, a finite element method has been developed that allows one to solve optimal control problems that have state discontinuities and/or discontinuities in the system equations as well as problems with control inequality constraints.

To address the future needs of real-time guidance for advanced launch systems, we present a four-state, two-stage model for the dynamics of mass, altitude, velocity, and flight-path angle. The angle of attack is the control. The results obtained by using the weak Hamiltonian finite element formulation for the four-state ALV model were compared with an essentially exact numerical method based on multiple shooting. The results show that the finite element method produces an accurate solution even when a small number of elements are taken. Furthermore, the finite element results were obtained within a short enough time to make the method a strong candidate for real-time optimal guidance. Finally, the algebraic equations that are derived for the finite element formulation are found without any numerical quadrature and can be easily programmed on a computer.

Acknowledgments

This work was supported by NASA Grant NAG-1-939 of which Daniel D. Moerder was the technical monitor. Technical discussions with Eric Corban are gratefully acknowledged.

References

[1]Hardtla, J. W., Piehler, M. J., and Bradt, J. E., "Guidance Requirements for Future Launch Vehicles," *Proceedings of the AIAA Guidance, Navigation, and Control Conference,* AIAA, New York, Aug. 1987.

[2]Hodges, D. H., and Bless, R. R., "Weak Hamiltonian Finite Element Method for Optimal Control Problems," *Journal of Guidance, Control, and Dynamics,* Vol. 14, No. 1, 1991, pp. 148–156.

[3]Petrov, Iu. P., *Variational Methods in Applied Optimum Control Theory,* translated by M. D. Friedman with the assistance of H. J. ten Zeldman, Academic, New York, 1968.

[4]Patten, W. N., "Near Optimal Feedback Control for Nonlinear Aerodynamic Systems with an Application to the High-Angle-of-Attack Wing Rock Problem," AIAA Paper 88-4052, Aug. 1988.

[5]Bryson, A. E., Jr., and Ho, Y.-C., *Applied Optimal Control,* Blaisdell, Waltham, MA, 1969, Chaps. 2 and 3.

[6]Bless, R. R., and Hodges, D. H., "Finite Element Solution of Optimal Control Problems with Control-State Inequality Constraints," *Journal of Guidance, Control, and Dynamics* (to be published).

[7]Jacobson, D. H., Lele, M. M., and Speyer, J. L., "New Necessary Conditions of Optimality for Control Problems with State-Variable Inequality Constraints," *Journal of Mathematical Analysis and Applications,* Vol. 35, No. 2, 1971, pp. 255–284.

[8]Gelfand, I. M., and Fomin, S. V., *Calculus of Variations,* Prentice-Hall, Englewood Cliffs, NJ, 1963.

[9]Valentine, F. A., "The Problem of Lagrange with Differential Inequalities as Added Side Conditions," *Contributions to the Calculus of Variations,* Chicago Univ. Press, Chicago, IL, 1937, pp. 407–448.

[10]Minzer, R. A., Reber, C. A., Jacchia, L. G., Huang, F. T., Cole, A. E., Kantor, A. J., Keneshea, T. J., Zimmerman, S. P., Forbes, J. M., "Defining Constants, Equations and Abbreviated Tables of the 1975 U.S. Standard Atmosphere," NASA TR R-459, May 1976.

[11]Pamadi, B., and Dutton, K., "An Aerodynamic Model for the Advanced Launch System Vehicle," NASA TM, under review, 1990.

[12]Duff, I. S., *Harwell Subroutine Library,* Computer Science and Systems Division, Harwell Lab., Oxfordshire, England, Feb. 1988, Chap. M.

[13]Bulirsch, R., "The Multiple Shooting Method for Numerical Solution of Nonlinear Boundary Value Problems and Optimal Control Problems," (in German), Carl-Cranz-Gesellschaft, Tech. Rept., Heidelberg, Germany, 1971.